Structural and metabolic cumulus cell alteration affects oocyte quality in underweight women

Hong Ji[1,2], Qing Zhang[1,2], Lu Ding[1,2], Rongjuan Chen[1,2], Fu Liu[3,*] and Ping Li[1,2,*]

[1]Department of Reproductive Medicine, Women and Children's Hospital, School of Medicine, Xiamen University, Zhenhai Road 10, 361003 Xiamen, Fujian Province, People's Republic of China; [2]Xiamen Key Laboratory of Reproduction and Genetics, Zhenhai Road 10, 361003, Xiamen, Fujian Province, People's Republic of China and [3]Department of Human Anatomy and Histoembryology, Xiamen Medical College, Guankou Middle Road 1999, 361023, Xiamen, Fujian Province, People's Republic of China

Summary

This study aimed to investigate the structural and metabolic changes in cumulus cells of underweight women and their effects on oocyte maturation and fertilization. The cytoplasmic ultrastructure was analyzed by electron microscopy, mitochondrial membrane potential by immunofluorescence, and mitochondrial DNA copy number by relative quantitative polymerase chain reaction. The expression of various proteins including the oxidative stress-derived product 4-hydroxynonenal (4-HNE) and autophagy and apoptosis markers such as Vps34, Atg-5, Beclin 1, Lc3-I, II, Bax, and Bcl-2 was assessed and compared between groups. Oocyte maturation and fertilization rates were lower in underweight women ($P < 0.05$), who presented with cumulus cells showing abnormal mitochondrial morphology and increased cell autophagy. Compared with the mitochondrial DNA copies of the control group, those of the underweight group increased but not significantly. The mitochondrial membrane potential was similar between the groups ($P = 0.8$). Vps34, Atg-5, Lc3-II, Bax, and Bcl-2 expression and 4-HNE levels were higher in the underweight group compared with the control group ($P < 0.01$); however, the Bax/Bcl-2 ratio was lower in the underweight group compared with the control group ($P = 0.031$). Additionally, Beclin 1 protein levels were higher in the underweight group compared with the control group but without statistical significance. In conclusion, malnutrition and other conditions in underweight women may adversely affect ovulation, and the development, and fertilization of oocytes resulting from changes to the intracellular structure of cumulus cells and metabolic processes. These changes may lead to reduced fertility or unsatisfactory reproduction outcomes in women.

Introduction

Research on the nutritional status and social determinants of women of reproductive age in China has revealed that the continuous development of the social economy has improved their quality of life (Dong and Yin, 2018). Nevertheless, the prevalence of underweight women of reproductive age that had been declining since 1991, has been increasing since 2004 (Song *et al.*, 2020). Chinese women are more inclined to weigh less and to have an adequate understanding of the harms of excess body weight; however, little information is known about the effects of low body weight on the health of this population. Women who visit assisted reproductive centres show great heterogeneity in terms of factors that may affect the outcome of assisted reproduction such as body weight and age (Mintziori *et al.*, 2020; Attali and Yogev, 2021). Doctors typically recommend that overweight women lose enough weight to fall within the normal range to achieve a more satisfactory pregnancy outcome (Hunter *et al.*, 2021). However, underweight women are not required to gain weight, and this suggests that medical staff may be paying insufficient attention to the effect of being underweight on pregnancy outcomes.

The fertility of underweight women is lower compared with that of normal-weight women, and being underweight may affect the hypothalamus–pituitary–ovary axis, possibly leading to ovulation that reduces fertility and the production of abnormal oocytes (Rich-Edwards *et al.*, 2002). Additionally, underweight women are more likely to experience poor outcomes during pregnancy (Boutari *et al.*, 2020). This suggests that the metabolism of underweight women may be disturbed, causing direct or indirect negative effects on oogenesis, ovulation, and even subsequent embryological development.

During the earliest stages of follicle development, granulosa cells expand and surround the oocytes. With the formation of the follicle lumen, granulosa cells gradually differentiate into two types: mural granulosa cells distributed around the follicle lumen, and cumulus cells surrounding the oocyte (Uyar *et al.*, 2013). Cumulus cells and the oocyte interact through

various methods such as gap junctions that transport proteins and paracrine factors (Aardema *et al.*, 2019). Moreover, cumulus cells deliver small molecules to the oocyte that participate in the maturation of its cytoplasm and nucleus and improve its developmental potential. Furthermore, the oocyte can regulate cumulus cell proliferation, diffusion, and metabolism by paracrine factors (Hirao, 2012). One of the major determinants of oocyte quality is the bidirectional interaction between cumulus cells and the oocyte itself. If the metabolic function of an oocyte is disrupted, its development and implant potential can be negatively affected both *in vivo* and *in vitro* (Richani *et al.*, 2021). Optimal glucose metabolism is one of the necessary conditions for an ovum to resume meiosis and cytoplasmic maturation, a process that depends on both the cumulus cells and the oocyte (Sutton-McDowall *et al.*, 2010). However, women with low body weight experience nutritional deficits and may have an abnormal glucose metabolism. If cumulus cells malfunction because of a lack of cellular energy, the growth and development of oocytes and early embryos will be affected, reducing their fertility (Liu *et al.*, 2018). Nonetheless, few studies have connected the apoptosis of cumulus cells to oocyte maturity and fertilization capacity.

Therefore, this study aimed to analyze the different parameters impacting the cumulus cells of underweight women. We analyzed the cytoplasmic ultrastructure, mitochondrial functionality, and levels of oxidative stress products in cumulus cells. Moreover, we quantified the expression of proteins associated with autophagy and apoptosis in cumulus cells. These data revealed the structural and metabolic changes in cumulus cells of underweight women, informing the discussion on the effect of these changes on the quality of oocytes.

Materials and methods

Ethical approval

All participants provided written informed consent for the use of their cumulus cells and clinical data for this study. This study was conducted in accordance with the Declaration of Helsinki (2013), and was approved by the Ethics Council of Human Research in Xiamen Maternal and Child Health Care Hospital, Fujian, China (Approval Number: KY-2020–065–01).

Selection of the study population (volume-exclusion criteria)

We limited this study to women undergoing *in vitro* fertilization and embryo transfer (IVF-ET) in our centre due to oviduct complications. The fertilization method was short-term IVF in all cases. According to a previous report on the Asian population (WHO Expert Consultation, 2004), the optimal body mass index (BMI) for women ranges from 18.5 kg/m^2 to 22.9 kg/m^2. We included women with a BMI within this range in the control group, while women with a BMI <18.5 kg/m^2 were included in the underweight group. Additionally, those with a BMI >22.9 kg/m^2 were excluded from this study.

Collection of relevant clinical data

Data regarding age, basal hormone levels of the patients [i.e. follicle-stimulating hormone (FSH) and anti-Müllerian hormone (AMH) levels on days 2 and 3 of menstruation], stimulation regimen of controlled ovarian hyperstimulation, sperm quality (concentration, motility, morphology) were collected from the electronic medical records database of our hospital.

In this study, we used the long-term protocol as the main regimen for controlled ovarian hyperstimulation, and only a few cases used the antagonist protocol and luteal phase protocol. A long-term protocol implies that patients were treated with the long-acting gonadotropin-releasing hormone agonist (GnRH-a) triptorelin (3.75 mg, IPSEN, France) by subcutaneous injection, and then exogenous gonadotrophins [recombinant FSH (rFSH): Gonal-F, 75 IU, Merck Serono, Switzerland] were administered by intramuscular injection, the gonadotrophin doses were based on the condition of the patients, their endogenous hormone levels and ultrasonography data. Human chorionic gonadotropin (hCG, Merck Serono, Switzerland) was injected when at least two follicles reached a diameter of 18 mm or three follicles reached a diameter of 17 mm. An antagonist protocol implies that patients were administered gonadotrophin between the third and fifth day of the menstrual cycle. The dosage was determined according to the criteria mentioned above (long-term protocol). When the dominant follicle was ≥14 mm in diameter, or E$_2$ ≥400 pg/ml, 0.25 mg/d GnRH antagonist (Cetrorelix Acetate, Swiss Serono company) was administered by subcutaneous injection until the day of triggering. The following procedures were similar to the long-term protocol. A luteal phase protocol implies that after the day of natural-cycle oocyte retrieval or the day of follicular rupture as monitored by B-ultrasonography, exogenous gonadotrophin (rFSH; Gonal-F, 75 IU, Merck Serono, Switzerland) was administered by intramuscular injection. The dosage was determined according to the criteria mentioned above (long-term protocol). When at least two follicles reached a diameter of 18 mm or three follicles reached a diameter of 17 mm, hCG was injected for the triggering of ovulation. Oocytes were retrieved 34 h after triggering ovulation by trans-virginal aspiration.

Data related to oocytes or embryo development including the number of oocytes, maturation, fertilization, 2PN fertilization, 2PN cleavage, available cleavage embryos, blastocyst formation, and available blastocysts were also collected. Among the above indicators, fertilization means 1PN (pronucleus), 2PN or ≥3PN can be observed in an oocyte at 17 ± 1 h post-insemination (at the time of checking for fertilization), or subsequent cleavage can be observed in a 0PN oocyte. The available cleavage embryos need to have 6–12 blastomeres and no more than 25% cell fragment at Day 3 (observation at 68 ± 1 h post-insemination). The available blastocysts must have at least three stages of blastocelic cavity, with inner cell masses rated as A or B and trophectoderm rated as A, B or C (Gardner and Schoolcraft, 1999; Alpha Scientists in Reproductive Medicine and ESHRE Special Interest Group of Embryology, 2011). As previously mentioned, all cases included in this study were inseminated using short-term IVF. In other words, the cumulus cells were removed 4–6 h after IVF insemination on the day of oocyte retrieval, and the second polar body of each oocyte was observed under a microscope to determine the fertilization status initially. In this process, the number of mature and immature oocytes can be recorded separately, as the morphology of each oocyte can be clearly observed under the microscope. Subsequently, the related rates were computed further using the following formulas:

$$\text{Oocyte maturation rate} = \text{number of mature oocytes}/ \text{number of oocytes retrieved} \times 100\% \quad (1)$$

$$\text{Fertilization rate} = \text{number of fertilized oocytes}/ \text{number of oocytes retrieved} \times 100\% \quad (2)$$

$$2PN\ fertilization\ rate = number\ of\ 2PN\ fertilized\ oocytes/number$$
$$of\ oocytes\ retrieved \times 100\% \quad (3)$$

$$2PN\ cleavage\ rate = number\ of\ 2PN\ cleavage\ oocytes/$$
$$number\ of\ 2PN\ fertilized\ oocytes \times 100\% \quad (4)$$

$$Available\ cleavage\ embryos\ rate =$$
$$number\ of\ available\ cleavage\ embryos/ \quad (5)$$
$$number\ of\ 2PN\ cleavage \times 100\%$$

$$Blastocyst\ formation\ rate = number\ of\ blastocyst\ formed/$$
$$number\ of\ cultured\ blastocysts \times 100\% \quad (6)$$

$$Available\ blastocysts\ rate = number\ of\ available\ blastocysts/$$
$$number\ of\ cultured\ blastocysts \times 100\% \quad (7)$$

Considering the effect of semen quality on fertilization in IVF, the concentration of semen and the proportion of sperm with progressive motility (PR) in this study were all in the normal range, and we did not strictly limit the proportion of sperm with normal morphology. Our assessment of semen quality was based on the 5th Edition of the WHO Laboratory Manual for the Examination and Treatment of Human Semen (World Health Organization, 2010)

Collection of cumulus cells

Cumulus–oocyte complexes (COCs) were isolated from follicular fluid, placed in a gamete buffer (Cook, McLean, Bloomington, USA), rinsed, and briefly cultured for 5–10 min. Gelatinous cumulus cells surrounding the COC were cut using two syringes, rinsed three times in normal saline, and washed to remove blood cells, tissue fragments, and residual follicular fluid components. Cumulus cell samples, obtained from multiple oocytes of the same patient, were stored with Fertilization Medium (Cook, McLean, Bloomington, USA) in a 5% CO_2 incubator at 37°C for 1–2 h before subsequent use.

Ultrastructural observations of cumulus cells

After three saline washes, cumulus cells were fixed in a 4% glutaraldehyde solution for 24 h. They were then rinsed three times with 0.1 M phosphate-buffered saline (PBS) at a pH of 7.4 followed by a secondary fixation in 1% osmium acid. Subsequently, they were dehydrated by an ethanol gradient, saturated with 100% acetone, and embedded in epoxy resin. Tissue sections 70-nm thick were spread on a copper screen and stained with lead citrate and uranium hydrogen acetate; the ultrastructure of cumulus cells was observed using a Tecnai G2 Spirit (FEI Company, Hillsboro, Ore, USA) transmission electron microscope.

Detection of mitochondrial membrane potential in cumulus cells (JC-1)

Cumulus cells were digested with trypsin for 1 min, washed twice with PBS (centrifuged at 352 rcf for 3 min), and incubated in Dulbecco's modified eagle medium with 10% fetal bovine serum for 6 h in a four-well plate. When the cells were adherent, the culture medium was changed. At 24 h later, the adherent cells were

Table 1. Primer sequences for the housekeeping and target genes

Name	Sequences
Act-F2	5′-GCCTCGCTGTCCACCTTCCA-3′
Actin-R3	5′-TTTTGTCAAGAAAGGGTGTAACGCA-3′
Act-TZ2	5′VIC-AAGCAGGAGTATGACGAGTCCG-MGB-3′
Primer MTF	5′-TGACCACCATCCTCCGTGAAAT-3′
Primer MTR	5′-ATCGTGATGTCTTATTTAAGGGGAA-3′
MT-TZ	5′-FAM-CAAGAGTGCTACTCTCCTCGCT-MGB-3′

stained for JC-1 following the instructions of the mitochondrial membrane potential detection kit (Beyotime, Shanghai, China).

The JC-1 stain working solution was prepared as follows: 50 µl of JC-1 stock solution (200×) was diluted with 8 ml of ultra-pure water (dilution ratio range: 1:160–200), fully dissolved, and mixed by a vortex mixer, placed at room temperature for 1–2 min, and mixed with 2 ml of JC-1 stain buffer stock solution (5×) to form the JC-1 stain working solution. For the buffer, 4 ml of ultra-pure water was mixed with 1 ml of buffer solution stock solution (5×) and the buffer was put in an ice bath. For staining the adherent cells with JC-1, PBS solution was used to wash the cells once, and the JC-1 staining working solution was added to cover the cell growth area; the cells were incubated in a 5% CO_2 incubator at 37°C for 20 min. After the supernatant was removed, cells were washed twice with JC-1 staining buffer working solution, and the appropriate amount of fresh cell culture medium was added. Finally, the red and green fluorescence intensities of the coloured cells were observed and recorded under a laser confocal microscope (LSM880, Zeiss, Oberkochen, Germany), and the ratio of red/green fluorescence intensity was calculated. In this analysis, red represented J aggregates that are indicative of high mitochondrial membrane potential and strong activity, whereas green represented the J monomer, indicative of low mitochondrial membrane potential and weakened activity. The cumulus cells of each patient were observed over three visual fields, and the mean fluorescence values were recorded. To summarize, this method allowed us to evaluate the mitochondrial functionality in cumulus cells.

Measuring mitochondrial DNA (mtDNA) from cumulus cells

The mitochondrial DNA (mtDNA) and internal reference genes in both groups of samples were quantified using relative fluorescence quantitative polymerase chain reaction (qPCR). After three washes with saline serum, the cumulus cells were stored at −40°C. The extraction of mtDNA was carried out according to the manufacturer's instructions using the Rapid Blood Genomic DNA Isolation Kit (Shanghai Biological Company, Shanghai, China). Then, the mtDNA was eluted in 200 µl of eluate. The primer design for qPCR was performed according to previous studies (Beijing Aegean Sea Music Technology Co., Ltd, 2018; Zhang *et al.*, 2021). Shanghai Shenggong Biological Company was commissioned to synthesize the primers. The primer sequences are presented in Table 1.

In this experiment, the reaction mixture contained a total volume of 10 µl, comprised of 5 µl of TaqMan Fast qPCR Master Mix (BBI, Roche, Switzerland), 0.2 µl each of forward and reverse primers for the target and β-actin genes, probe in 0.2 µl, ddH_2O 3.4 µl, and 1 µl of the template. Each primer and the probe were diluted to a concentration of 10 µM (10 µmol/l). The 384-well plate carrying the qPCR samples was placed in LightCycler480 II

Table 2. Baseline data, gamete and embryo development details of both groups of participants

	Control	Underweight group	X2/t/Z	P
n	21	20		
Age (years)	30.71 ± 4.95	29.85 ± 3.30	0.654	0.517
BMI[a]	20.3 (19.45–21.65)	17.55 (16.43–18)	5.482	<0.001*
FSH[a]	6.98 (6.23–8.90)	7.26 (6.25–9.50)	0.522	0.602
AMH[a]	5.31 (1.93–13.07)	3.39 (2.09–5.52)	1.252	0.211
Regime of controlled ovarian hyperstimulation				
Long-term protocol	18	14	3.478	0.176
Antagonist protocol	3	3		
Luteal phase protocol	0	3		
No. of oocytes retrieved	14.14 ± 6.98	13.20 ± 6.63	0.151	0.700
Concentration of the sperm[a]	68 (35–110)	56.6 (43.5–87.75)	−0.065	0.948
PR sperm (%)	45.95 ± 11.36	43.05 ± 10.61	1.234	0.273
Normal sperm morphology (%)[a]	12 (6–16)	12 (8.5–16)	−0.27	0.787
Oocyte maturation rate	93.3% (277/297)	87.5% (231/264)	5.432	0.020*
Fertilization rate	86.2% (256/297)	78.4% (207/264)	5.877	0.015*
2PN fertilization rate	65% (193/297)	65.5% (173/264)	0.018	0.892
2PN cleavage rate	96.9% (187/193)	98.3% (170/173)	0.719	0.397
Available cleavage embryo rate	79.1% (148/187)	84.1% (143/170)	1.462	0.227
Blastocyst formation rate	67.3% (115/171)	69.9% (102/146)	0.249	0.618
Available blastocyst rate	50.9% (87/171)	50% (73/146)	0.024	0.876

[a]Non-normally distributed data, a non-parametric test was used; *$P < 0.05$.
AMH, anti-Müllerian hormone; BMI, body mass index; PR sperm, progressive sperm.

(Roche, Switzerland) for real-time PCR. The cycling conditions were set to the following parameters: initial steps: 94°C for 3 min, followed by 45 cycles of 94°C for 5 s, 57°C for 15 s, and 72°C for 30 s.

Expression of protein markers of oxidative stress, autophagy, and apoptosis in cumulus cells

To prepare the cell lysates, the cumulus cells were lysed with the radioimmunoprecipitation assay lysis buffer (50 mM Tris-Cl, pH 7.4, 150 mM NaCl, 0.1% SDS, 1% NP-40, 1% sodium deoxycholate, 1 mM phenylmethyl-sulfurylfluoride, 1 mg/ml pepstatin, 1 mg/ml leupeptin, 1 mg/ml aprotinin, 1 mM NaF, and 1 mM Na_3VO_4), while maintained on ice for 30 min. After being homogenized, the samples were centrifuged at 15294 rcf at 4°C for 15 min. All protein concentrations were determined using the BCA Protein Assay kit (Beyotime, Shanghai, China). Equal amounts of proteins (30 to 40 μg) were separated by electrophoretic sodium dodecyl sulfate-polyacrylamide gel electrophoresis and then transferred to a 0.22-μm pore size nitrocellulose blotting membrane (Pall Life Sciences, USA). After being blocked with 5% skimmed milk, the membranes were incubated overnight with primary antibodies (Atg5, Lc3-I/II, Beclin 1, Cell Signaling Technologies, Danvers, Massachusetts, USA; Vps34, ThermoFisher Scientific, Waltham, MA, USA; 4-HNE, Abcam, Cambridgeshire, UK; Bax, Bcl-2, Beyotime, Shanghai, China), then incubated with horseradish peroxidase-conjugated secondary antibodies (ZSGB-BIO, Beijing, China), the immunoreactive bands were subsequently visualized with enhanced chemiluminescence, and the band intensity was quantified.

Statistical analysis

Each experiment was repeated more than three times separately. Statistical analyses were performed with Statistical Package for the Social Sciences (SPSS) software version 19.0 (IBM Corp., Armonk, NY, USA). Normally distributed data were analyzed using the Shapiro–Wilk test and expressed as mean ± standard deviation. Non-normally distributed data were expressed as median with interquartile range. Comparisons between groups were analyzed with non-parametric tests for two independent samples. Countable data were analyzed using the chi-squared test. Finally, the differences in protein expression levels between the two groups were determined using the *t*-test for independent samples. Statistical significance was set at $P < 0.05$.

Results

Basic patient information and gamete/embryo data

In this study, there were 20 and 21 participants in the underweight and control groups, respectively. Apart from BMI ($P < 0.001$), there were no statistical differences in age, basal FSH, AMH levels, regimen distribution of controlled ovarian hyperstimulation, number of oocytes retrieved, sperm concentration, the proportion of PR sperm and the proportion of normal sperm morphology between the two groups. The oocyte maturation and fertilization rates showed statistically significant differences between groups ($P < 0.05$), whereas the rates of 2PN fertilization, 2PN cleavage, available cleavage embryos, blastocyst formation, and available blastocyst did not have statistically significant differences between the two groups (Table 2).
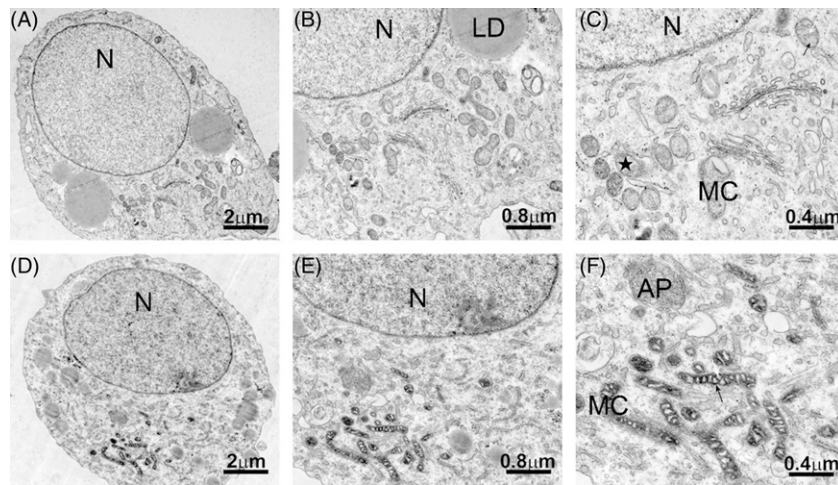
Figure 1. Electron micrographs of the ultrastructure of cumulus cells in the underweight and control groups. (A–C) Ultrastructure of cumulus cells under different magnifications in the control group. (D–F) Ultrastructure of cumulus cells under different magnifications in the underweight group. Micrographs (A) and (D) have been magnified 3000 times (×3000), (B) and (E) have been magnified 5000 times (×5000), while (C) and (F) have been magnified 10,000 times (×10,000). AP, autophagosomes; LD, lipid droplet; MC, mitochondria; N, nucleus. The white arrow refers to cristae, the black arrow refers to the matrix, and ★ indicates a transverse section of mitochondria.
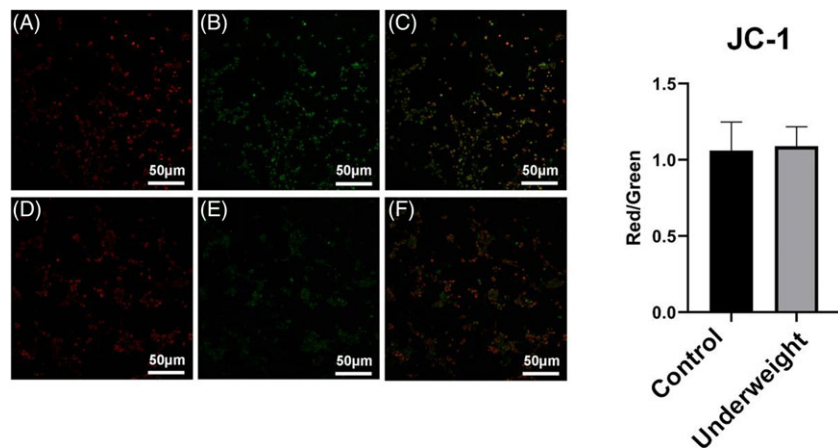
Figure 2. Mitochondrial membrane potentials of cumulus cells in the underweight and control groups. (A–C) Mitochondrial membrane potential map of the cumulus cells in the control group. (D–F) Mitochondrial membrane potential map of the cumulus cells in the underweight group. (A) and (D) show the red channel, (B) and (E) show the green channel, and (C) and (F) show the superimposition of the two channels. The bar graph on the right shows the comparison of the fluorescence ratio values of each channel between the two groups.

Cytoplasmic ultrastructure of cumulus cells

After fixing, sectioning, and staining the two groups of cumulus cell samples, we observed the intracellular ultrastructure through electron microscopy and found differences in the morphology of mitochondria and cytoplasmic autophagosomes. The mitochondrial cristae of the underweight group were swollen and empty, while the matrix was trachychromatic and showed a zebra-like mitochondrial pattern (present in 60.9% of the cell samples in this group). Moreover, a higher number of autophagosomes (i.e. autophagic lysosomes) could be seen in the cytoplasm of the underweight group. By contrast, in most samples of the control group (77.8%), the mitochondrial cristae were clear and the matrix was normal (hypochromatic). Furthermore, a lower number of autophagosomes was seen in the cytoplasm of the control group (Figure 1).

Mitochondrial membrane potential in cumulus cells

After a brief *in vitro* culture of cumulus cells in both groups, we used the mitochondrial membrane potential detection kit and assessed the function of mitochondria by analyzing the differences in mitochondrial activity. Fluorescence microscopy showed that, although the red/green fluorescence ratio of the cells in the underweight group was higher compared with that of the control group, the difference was not statistically significant ($P = 0.8$).

These results indicated that the mitochondrial function was similar between the two groups after *in vitro* culture (Figure 2).

Relative quantification of mitochondrial DNA (mtDNA)

We performed relative quantification of mtDNA in both groups of samples using qPCR, and these results are presented as fold-change values. Our data showed that the median fold-change value for mtDNA of the underweight group was 1.4489, whereas that of the control group was 1.1221. The fold-change was greater in the underweight group compared with the control group; however, this difference was not statistically significant ($P = 0.087$; Figure 3).

Differences in oxidative stress, autophagy, and apoptosis-related proteins in cumulus cells

To analyze the occurrence of biological events, such as oxidative stress, autophagy, and apoptosis in cumulus cells, we selected 4-HNE, a product of mitochondrial oxidative stress, and various autophagy and apoptosis-related proteins including Vps34, Atg-5, Beclin 1, Lc3-II, Bax, and Bcl-2 as target proteins. Protein expression levels in cumulus cells were detected by western blotting. 4-HNE expression was higher in the underweight group compared with the control group ($P = 0.007$). Protein expression levels of Vps34, Atg-5, and Lc3-II were higher in the underweight group compared with the control group ($P = 0.002$, $P = 0.007$, and
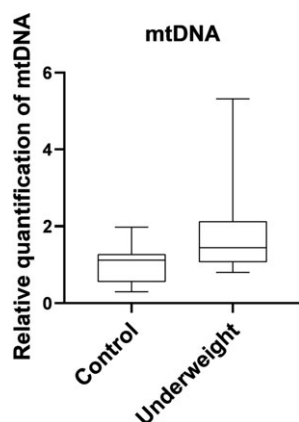
Figure 3. Relative quantification of mitochondrial DNA in underweight and control groups. mtDNA, mitochondrial DNA.

$P = 0.005$, respectively). The underweight group also showed an increase in Beclin 1 protein expression; however, the difference between the groups was not statistically significant ($P = 0.634$). Finally, Bax and Bcl-2 expression levels were significantly higher in the underweight group compared with the control group. However, the Bax/Bcl-2 ratio was significantly lower in the underweight group compared with the control group ($P = 0.031$; Figure 4).

Discussion

In this study, baseline data regarding patients who underwent IVF-ET in both groups were not significantly different, making the groups suitable for comparison. As shown in Table 2, the oocyte maturation and fertilization rates of patients in the underweight group were significantly lower compared with those in the control group. These data suggest that oocytes of underweight women may have experienced developmental arrest, delayed maturation, or other abnormalities that may have affected fertilization.

In the female reproductive system, the follicle microenvironment is composed of follicular fluid, oocytes, and cumulus cells (Hennet and Combelles, 2012). Furthermore, communication between different components plays a key role in subsequent development during oocyte maturation (Turathum et al., 2021). The oocyte discharge, one of the main factors for correct oocyte development, also affects natural female fertility and the potential results of assisted reproductive pregnancy (Dumesic et al., 2015; Biase and Kimble, 2018). Being underweight may be related to malnutrition (Lahmann et al., 2016); therefore, malnutrition may lead to oxidative stress and mitochondrial damage in heart cells and surrounding tissues (Ferreira et al., 2016). Moreover, malnutrition may affect the energy metabolism of the follicular microenvironment, altering the structure of oocytes and cumulus cells (Chen et al., 2012). When nutrients are insufficient, cumulus cell mitochondria are the first to suffer quantitative and functional changes. As mitochondria are the most important source of cellular energy, these adverse changes may cause a physiological dysfunction in cumulus cells and a loss of cell homeostasis, due to an imbalance in pro- and antioxidant compounds. Consequently, oocyte maturation, ovulation, and fertility would be inevitably altered (Da Broi et al., 2018).

Oxidative metabolism in eukaryotes mainly occurs in the mitochondria (Papa et al., 2012). This organelle is where sugar, fat,

and amino acids are eventually oxidized to release energy. The cristae in the cytoplasm of normal mitochondria should be relatively clear; in contrast, the underlying matrix of the inner membrane should be lightly stained to ensure that the mitochondria can undertake additional biochemical reactions. However, the ultrastructure of cumulus cells in underweight women showed that the mitochondrial cristae of some of their cells were swollen and vacuolar, and the underlying matrix of the inner membrane was deeply stained and even showed a 'zebra-crossing' pattern (Figure 1). Considering that in addition to providing energy to cells, mitochondria also participate in the metabolic regulation of cell signalling, maintenance of calcium homeostasis, cell proliferation, differentiation, and apoptosis (Annesley and Fisher, 2019), these changes at the mitochondrial level may have negative effects on the activity and function of cumulus cells (Kansaku et al., 2018).

The membrane potential of the mitochondria is considered a common and important indicator of its physiological and functional status. Mitochondrial structures with higher membrane potential are also considered complete and functionally active (Perry et al., 2011). In a healthy mitochondrial membrane, numerous negative charges are common. Moreover, when the membrane potential is high, the fluorescent probe JC-1 can accumulate in the mitochondrial matrix, forming a polymer and emitting a bright red fluorescence (Perelman et al., 2012). In contrast, when the membrane potential drops, the mitochondrial inner membrane permeability increases, leading to depolarization. In this case, JC-1 cannot accumulate and only exists as a monomer that emits green fluorescence. The ratio of red/green fluorescence is a measure of change in mitochondrial activity. Contrary to our expectations, Figure 2 shows that the red/green fluorescence ratio of the underweight group was slightly higher compared with that of the control group; however, this difference between the two groups was not significant. Similarly, as seen in Figure 3, the mtDNA copy number of the underweight group was also higher compared with that of the control group. As shown in Figure 1, some of the mitochondria in the underweight group indeed underwent morphological changes. Therefore, we hypothesized that cells of the underweight group may have an increased mitochondrial proliferation rate that may not be synchronized with cell proliferation, to maintain energy supply. Moreover, minor differences can also be due to the possibility that mitochondrial membrane integrity and mtDNA copy number may also be affected by various external factors, such as transient in vitro culture or other compensatory mechanisms in the cell, especially in the underweight group. An earlier report (Desquiret-Dumas et al., 2017) showed that BMI was negatively correlated with mtDNA copy number, similar to our results.

As the primary site of aerobic respiration within the cell, healthy mitochondria constantly produce and decompose reactive oxygen species (ROS), regulate their balance and concentration, and ensure the correct functioning of the respiratory electron transport chain. Therefore, mitochondria with abnormal structures may lose their capacity to maintain this balance, and begin accumulating ROS within the cell and releasing various oxidative stress products. 4-HNE is an endogenous oxidative stress marker derived from the lipid peroxidation process of polyunsaturated fatty acids in different tissues and cells (Li et al., 2022). Its production in mitochondria leads to oxidative damage at a cellular level (Sharma et al., 2022). Therefore, dysregulation of intracellular ROS production results in the expression of 4-HNE. ROS could regulate changes in mtDNA copy number, and the accumulation of ROS may induce a compensatory increase in mtDNA to counter the
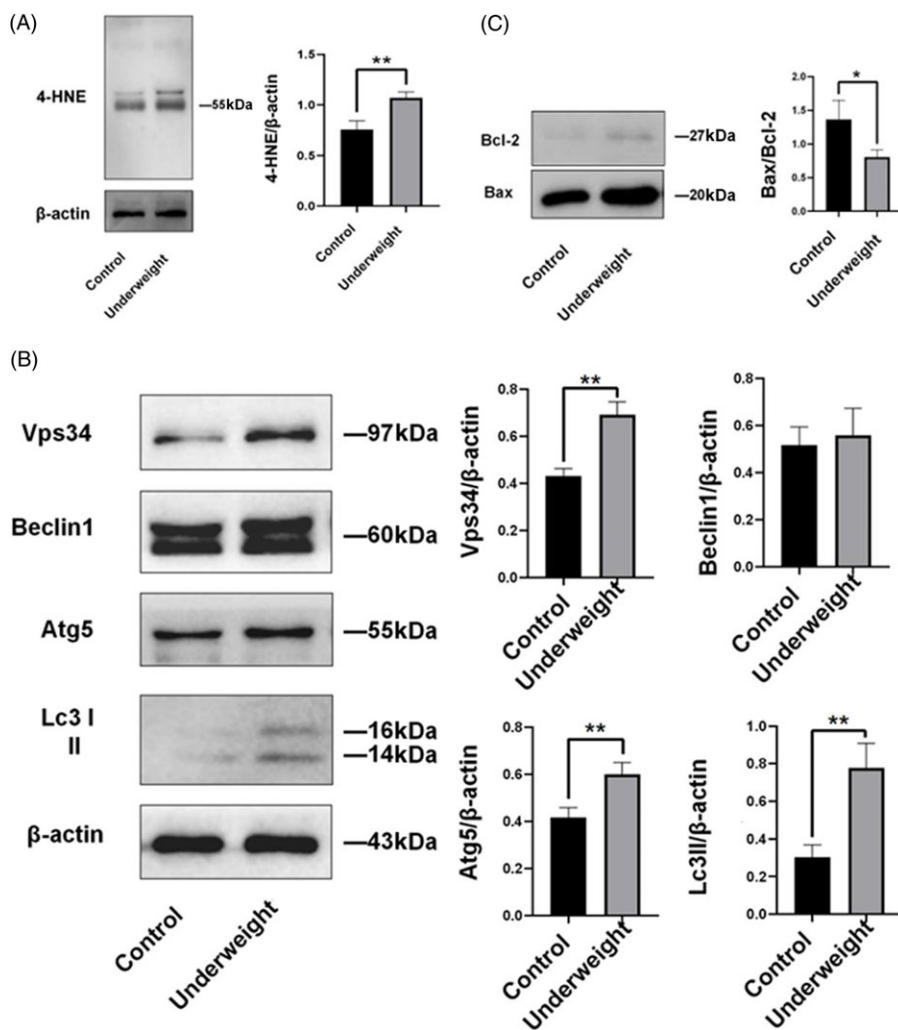
Figure 4. Oxidative stress, autophagy, and apoptosis-related protein expression quantified by western blotting in the underweight and control groups. (A) Expression of the oxidative stress product 4-HNE. (B) Expression of autophagy-related proteins. (C) Expression of apoptosis-related proteins. *$P < 0.05$, **$P < 0.01$.

adverse effects of ROS (Skuratovskaia *et al.*, 2018). As shown in Figure 4, the expression of 4-HNE in the underweight group was significantly higher compared with that in the control group. This result indicates that oxidative stress was enhanced, and that ROS had accumulated in cells, and this may explain the slight increase in mtDNA copy number in this group.

Autophagy is a stress-induced biological process in which cells degrade their internally damaged organelles, such as mitochondria and endoplasmic reticulum fragments, large misfolded protein complexes, and pathogens (Mizushima and Komatsu, 2011), playing a key role in the maintenance of cellular homeostasis. as nutrients and energy consumed during autophagy can be reused in various cellular activities, the cell can survive under stressful conditions. Therefore, in a scenario in which there is a lack of nutrients and energy in the mitochondria, the continuous synthesis of mtDNA requires autophagy and other metabolites to prevent excessive ROS, alleviate oxidative damage, and help cells and mitochondria to maintain metabolic homeostasis (Pyo *et al.*, 2013; Medeiros *et al.*, 2018; Medeiros and Graef, 2019). The autophagosome usually performs autophagy. Autophagosomes, also known as autophagy lysosomes, consist of a double membrane that surrounds a small part of the cytoplasm that has the capacity to digest its own contents enzymatically (Hollenstein and Kraft, 2020). When cells undergo pathological changes (i.e. atrophy), autophagosome numbers increase. In addition to injury, the degree

of cellular autophagy may also be affected by the nutritional conditions of the body (Corsetti *et al.*, 2021). Therefore, autophagy is inhibited in normal nutritional conditions; however, it is promoted when nutrition is insufficient – a condition that underweight women may face – by increasing the number or activity of autophagosomes (Cuervo and Macian, 2012).

In addition to the morphological changes in mitochondria, we observed higher autophagosome numbers in cumulus cells in the underweight group compared with the control group (Figure 1). Based on our electron microscopy results illustrated in Figure 1, we determined the expression levels of autophagy-related proteins from cumulus cells of both groups (Figure 4). The results showed that the expression of autophagy-related proteins Vps34, Atg-5, and Lc3II was significantly higher in the underweight group compared with the control group, and the expression of Beclin 1 was slightly higher in the underweight group (although not significantly different), indicating an increase in the number or activity of autophagosomes in this group. We speculate that this result may be related to the occurrence of malnutrition in some underweight women.

Type II cellular autophagy cooperates with apoptosis to regulate programmed cell death (D'Arcy, 2019). Conversely, in some cases, autophagy can inhibit apoptosis, leading to cell survival. Generally, autophagy induces cell death, either by cooperating with apoptosis or inducing it as a backup mechanism when apoptotic mechanisms

fail to be activated (Barth *et al.*, 2010). The two mechanisms can be activated by multiple stress stimuli. Moreover, they share multiple regulatory molecules and even reciprocally coordinate their bidirectional transformation (Maiuri *et al.*, 2007). In this context, the Bcl-2 protein family plays a critical role in the dual regulation of apoptosis and autophagy (Boldura *et al.*, 2021). In this study, we measured the expression of the proapoptotic protein Bax and antiapoptotic protein Bcl-2 in cumulus cells and calculated the Bax/Bcl-2 ratio (Figure 4). Notably, this ratio was lower in underweight women, indicating that antiapoptotic factors may play a larger role in this group compared with proapoptotic factors. Furthermore, the absolute expression of Bax and Bcl-2 was significantly higher in underweight women. These data suggest that the cumulus cells in these patients were under some type of stress (i.e. nutrient deprivation), and, in this context, the cells were trying to enhance their autophagic activity to preserve themselves. Nevertheless, these cells showed a clear enhancement of apoptotic processes.

Few studies have connected the apoptosis of cumulus cells to oocyte maturity and fertilization capacity (Høst *et al.*, 2000). In this study, the poor quality of the oocytes obtained from underweight women was mainly reflected in the significantly lower oocyte maturation and fertilization rates compared with those of the control group participants (Table 2). Considering the bidirectional regulation operating between cumulus cells and oocytes, we speculate that the oocyte maturation events, and apoptotic processes of cumulus cells are not only related but may also reciprocally affect each other. When cumulus cells undergo apoptosis and cannot maintain an effective dialogue with the oocyte, the oocyte cannot successfully complete nuclear and cytoplasmic maturation (Liu *et al.*, 2015). In contrast, when the oocyte does not mature for various reasons, the survival of cumulus cells is also threatened. Therefore, both autophagy and apoptosis determine the final fate of cumulus cells. This evidence, combined with Bax and Bcl-2 data (Figure 4), supports the notion that, although the oocyte maturity is low in underweight women, Bcl-2 may eventually lead to a stronger antiapoptotic effect because of the balance between autophagy and apoptosis response in cumulus cells. Indeed, the overall integrity of the cells is maintained but is inevitably accompanied by some impaired functions that may partially explain the results regarding oocyte quality.

In cumulus cells of the underweight group, we observed undesirable changes in mitochondrial morphology, a slight increase in their mtDNA copy number and mitochondrial membrane potential, and significantly elevated 4-HNE levels. These cells initiate both autophagy and apoptosis, increasing the number of autophagosomes and upregulating Vps34, Beclin 1, Atg-5, and Lc3 expression. Moreover, the expression of the proapoptotic factor Bax and the antiapoptotic factor Bcl-2 was significantly upregulated, and the effect of the latter was relatively enhanced in underweight women.

This study has some limitations. First, when analyzing the mitochondrial membrane potential, we used the same cell medium *in vitro*, and this allowed cells from the underweight group to receive adequate nutrition and energy supply. We then tested JC-1 once the cells were attached. These cells were subjected to natural selection. A previous report found that cumulus cell mitochondrial function was improved when the cells received adequate nutrients (Silva *et al.*, 2019). Therefore, we speculate that the reason for the lack of a significant difference in the results of JC-1 detection between the two groups was because of cellular compensatory mechanisms and the above factors. Stronger conclusions may be obtained if freshly collected cumulus cells were to be promptly counted by flow cytometry. Second, different ovulation induction regimens may lead to different effects on cumulus cells (Azizollahi *et al.*, 2021); however, as this study did not impose strict restrictions on the enrolment conditions of patients due to the small number of total cases available to us, the bias of some confounding factors on the experimental results cannot be excluded. Third, due to the limitation of experimental conditions, this study mainly focused on the ultrastructure of cumulus cells and their protein levels associated with different biochemical events. More detailed and in-depth research was not conducted at the cellular and molecular levels. Changes in the follicular microenvironment in underweight women, such as changes in the composition of follicular fluid and signal transmission between cumulus cells and oocytes, require a more in-depth analysis in the future.

Regarding clinical practice, we need to reconsider the following question: independent of the type of conception (natural or assisted), will gaining weight in preparation for pregnancy improve fertility in underweight women? Currently, several studies support this approach. For instance, appropriate weight gain before pregnancy in underweight patients could achieve pregnancy outcomes similar to those of patients with normal weight (Liu *et al.*, 2020). A preclinical study in mice (Zhu *et al.*, 2020) found that, after the surgical removal of white adipose tissue from around the ovaries, these animals showed follicular dysplasia, increased atresia, reduction of sex hormone levels in serum, and changes in the expression of genes related to follicle development. However, after receiving better culture conditions, the subsequent development of the embryo was not further affected (Zhu *et al.*, 2020). These results support a prompt improvement of the poor nutritional status in underweight women, demonstrating that a proper amount of body fat may be beneficial to reproductive function. Therefore, an optimal weight management strategy for women should encompass both overweight/obese and underweight patients, encouraging and helping them to adopt a healthy lifestyle, so as to adjust their BMI to within a suitable range for a more favourable metabolic foundation for natural conception or assisted reproduction.

To summarize, the results of this study suggested that underweight women have a lower rate of oocyte maturation and fertilization in comparison with women with a normal BMI. Additionally, levels of oxidative stress products and autophagy-related and apoptosis-related proteins were significantly higher, cumulus cells with abnormal mitochondrial morphology were present, and cell autophagy levels increased in underweight women.

no role in the study design, data collection, data analysis, interpretation of data, the writing of the report, and the decision to submit the article for publication.

Competing interests. The authors declare no conflicts of interest.

Ethical statement. The authors assert that all procedures contributing to this work complied with the ethical standards of the relevant national and institutional committees on human experimentation and with the Helsinki Declaration of 1975, as revised in 2008.

References

Aardema, H., van Tol, H. T. A. and Vos, P. L. A. M. (2019). An overview on how cumulus cells interact with the oocyte in a condition with elevated NEFA levels in dairy cows. *Animal Reproduction Science*, **207**, 131–137. doi: 10.1016/j.anireprosci.2019.06.003

Alpha Scientists in Reproductive Medicine and ESHRE Special Interest Group of Embryology (2011). The Istanbul consensus workshop on embryo assessment: Proceedings of an expert meeting. *Human Reproduction*, **26**(6), 1270–1283. doi: 10.1093/humrep/der037

Annesley, S. J. and Fisher, P. R. (2019). Mitochondria in health and disease. *Cells*, **8**(7), 680. doi: 10.3390/cells8070680

Attali, E. and Yogev, Y. (2021). The impact of advanced maternal age on pregnancy outcome. *Best Practice and Research. Clinical Obstetrics and Gynaecology*, **70**, 2–9. doi: 10.1016/j.bpobgyn.2020.06.006

Azizollahi, S., Bagheri, M., Haghollahi, F., Mohammadi, S. M. and Hossein Rashidi, B. H. (2021). Clinical and molecular effects of GnRH agonist and antagonist on the cumulus cells in the *in vitro* fertilization cycle. *International Journal of Fertility and Sterility*, **15**(3), 202–209. doi: 10.22074/IJFS.2020.136161.1012

Barth, S., Glick, D. and Macleod, K. F. (2010). Autophagy: Assays and artifacts. *Journal of Pathology*, **221**(2), 117–124. doi: 10.1002/path.2694

Biase, F. H. and Kimble, K. M. (2018). Functional signaling and gene regulatory networks between the oocyte and the surrounding cumulus cells. *BMC Genomics*, **19**(1), 351. doi: 10.1186/s12864-018-4738-2

Boldura, O. M., Marc, S., Otava, G., Hutu, I., Balta, C., Tulcan, C. and Mircu, C. (2021) Utilization of rosmarinic and ascorbic acids for maturation culture media in order to increase sow oocyte quality prior to IVF. *Molecules*, **26**(23), 7215. doi: 10.3390/molecules26237215

Boutari, C., Pappas, P. D., Mintziori, G., Nigdelis, M. P., Athanasiadis, L., Goulis, D. G. and Mantzoros, C. S. (2020). The effect of underweight on female and male reproduction. *Metabolism: Clinical and Experimental*, **107**, 154229. doi: 10.1016/j.metabol.2020.154229

Chen, T. Y., Stott, P., Athorn, R. Z., Bouwman, E. G. and Langendijk, P. (2012). Undernutrition during early follicle development has irreversible effects on ovulation rate and embryos. *Reproduction, Fertility, and Development*, **24**(6), 886–892. doi: 10.1071/RD11292

Corsetti, G., Pasini, E., Romano, C., Chen-Scarabelli, C., Scarabelli, T. M., Flati, V., Saravolatz, L. and Dioguardi, F. S. (2021). How can malnutrition affect autophagy in chronic heart failure? Focus and perspectives. *International Journal of Molecular Sciences*, **22**(7), 3332. doi: 10.3390/ijms22073332

Cuervo, A. M. and Macian, F. (2012). Autophagy, nutrition and immunology. *Molecular Aspects of Medicine*, **33**(1), 2–13. doi: 10.1016/j.mam.2011.09.001

D'Arcy, M. S. (2019). Cell death: A review of the major forms of apoptosis, necrosis and autophagy. *Cell Biology International*, **43**(6), 582–592. doi: 10.1002/cbin.11137

Da Broi, M. G., Jordão, A. A., Jr., Ferriani, R. A. and Navarro, P. A. (2018). Oocyte oxidative DNA damage may be involved in minimal/mild endometriosis-related infertility. *Molecular Reproduction and Development*, **85**(2), 128–136. doi: 10.1002/mrd.22943

Desquiret-Dumas, V., Clément, A., Seegers, V., Boucret, L., Ferré-L'Hotellier, V., Bouet, P. E., Descamps, P., Procaccio, V., Reynier, P. and May-Panloup, P. (2017). The mitochondrial DNA content of cumulus granulosa cells is linked to embryo quality. *Human Reproduction*, **32**(3), 607–614. doi: 10.1093/humrep/dew341

Dong, C. X. and Yin, S. A. (2018). The ten-year retrospect of nutrition and health status of pregnant women in China. *Zhonghua Yu Fang Yi Xue Za Zhi [Chinese Journal of Preventive Medicine]*, **52**(1), 94–100. doi: 10.3760/cma.j.issn.0253-9624.2018.01.019

Dumesic, D. A., Meldrum, D. R., Katz-Jaffe, M. G., Krisher, R. L. and Schoolcraft, W. B. (2015). Oocyte environment: Follicular fluid and cumulus cells are critical for oocyte health. *Fertility and Sterility*, **103**(2), 303–316. doi: 10.1016/j.fertnstert.2014.11.015

Ferreira, D. J. S., da Silva Pedroza, A. A., Braz, G. R. F., da Silva-Filho, R. C., Lima, T. A., Fernandes, M. P., Doi, S. Q. and Lagranha, C. J. (2016). Mitochondrial bioenergetics and oxidative status disruption in brainstem of weaned rats: Immediate response to maternal protein restriction. *Brain Research*, **1642**, 553–561. doi: 10.1016/j.brainres.2016.04.049

Gardner, D. K. and Schoolcraft, W. B. (1999). *In vitro* culture of human blastocysts. In R. Jansen & D. Mortimer (Eds.), *Toward reproductive certainty: Fertility and genetics beyond* 1999 (pp. 378–388). Parthenon Publishing Group.

Hennet, M. L. and Combelles, C. M. H. (2012). The antral follicle: A microenvironment for oocyte differentiation. *International Journal of Developmental Biology*, **56**(10–12), 819–831. doi: 10.1387/ijdb.120133cc

Hirao, Y. (2012). Oocyte growth *in vitro*: Potential model for studies of oocyte-granulosa cell interactions. *Reproductive Medicine and Biology*, **11**(1), 1–9. doi: 10.1007/s12522-011-0096-3

Hollenstein, D. M. and Kraft, C. (2020). Autophagosomes are formed at a distinct cellular structure. *Current Opinion in Cell Biology*, **65**, 50–57. doi: 10.1016/j.ceb.2020.02.012

Høst, E., Mikkelsen, A. L., Lindenberg, S. and Smidt-Jensen, S. (2000). Apoptosis in human cumulus cells in relation to maturation stage and cleavage of the corresponding oocyte. *Acta Obstetricia et Gynecologica Scandinavica*, **79**(11), 936–940. doi: 10.3109/00016340009169238

Hunter, E., Avenell, A., Maheshwari, A., Stadler, G. and Best, D. (2021). The effectiveness of weight-loss lifestyle interventions for improving fertility in women and men with overweight or obesity and infertility: A systematic review update of evidence from randomized controlled trials. *Obesity Reviews*, **22**(12), e13325. doi: 10.1111/obr.13325

Kansaku, K., Munakata, Y., Itami, N., Shirasuna, K., Kuwayama, T. and Iwata, H. (2018). Mitochondrial dysfunction in cumulus–oocyte complexes increases cell-free mitochondrial DNA. *Journal of Reproduction and Development*, **64**(3), 261–266. doi: 10.1262/jrd.2018-012

Lahmann, N. A., Tannen, A. and Suhr, R. (2016). Underweight and malnutrition in home care: A multicenter study. *Clinical Nutrition*, **35**(5), 1140–1146. doi: 10.1016/j.clnu.2015.09.008

Li, Y., Zhao, T., Li, J., Xia, M., Li, Y., Wang, X., Liu, C., Zheng, T., Chen, R., Kan, D., Xie, Y., Song, J., Feng, Y., Yu, T. and Sun, P. (2022). Oxidative stress and 4-hydroxy-2-nonenal (4-HNE): implications in the pathogenesis and treatment of aging-related diseases. *Journal of Immunology Research*, **2022**, 2233906. doi: 10.1155/2022/2233906

Liu, S., Jiang, L., Zhong, T., Kong, S., Zheng, R., Kong, F., Zhang, C., Zhang, L. and An, L. (2015). Effect of acrylamide on oocyte nuclear maturation and cumulus cells apoptosis in mouse *in vitro*. *PLOS ONE*, **10**(8), e0135818. doi: 10.1371/journal.pone.0135818

Liu, Q., Zhang, J., Wen, H., Feng, Y., Zhang, X., Xiang, H., Cao, Y., Tong, X., Ji, Y. and Xue, Z. (2018). Analyzing the transcriptome profile of human cumulus cells related to embryo quality via RNA sequencing. *BioMed Research International*, **2018**, 9846274. doi: 10.1155/2018/9846274

Liu, L. Y., Zafman, K. B. and Fox, N. S. (2020). Weight gain and pregnancy outcomes in underweight women with twin gestations. *Journal of Maternal-Fetal and Neonatal Medicine*, **33**(17), 2877–2881. doi: 10.1080/14767058.2018.1562544

Maiuri, M. C., Zalckvar, E., Kimchi, A. and Kroemer, G. (2007). Self-eating and self-killing: Crosstalk between autophagy and apoptosis. *Nature Reviews. Molecular Cell Biology*, **8**(9), 741–752. doi: 10.1038/nrm2239

Medeiros, T. C. and Graef, M. (2019). Autophagy determines mtDNA copy number dynamics during starvation. *Autophagy*, **15**(1), 178–179. doi: 10.1080/15548627.2018.1532263

Medeiros, T. C., Thomas, R. L., Ghillebert, R. and Graef, M. (2018). Autophagy balances mtDNA synthesis and degradation by DNA polymerase POLG during starvation. *Journal of Cell Biology*, **217**(5), 1601–1611. doi: 10.1083/jcb.201801168

Mintziori, G., Nigdelis, M. P., Mathew, H., Mousiolis, A., Goulis, D. G. and Mantzoros, C. S. (2020). The effect of excess body fat on female and male reproduction. *Metabolism: Clinical and Experimental*, **107**, 154193. doi: 10.1016/j.metabol.2020.154193

Mizushima, N. and Komatsu, M. (2011). Autophagy: renovation of cells and tissues. *Cell*, **147**(4), 728–741. doi: 10.1016/j.cell.2011.10.026

Papa, S., Martino, P. L., Capitanio, G., Gaballo, A., De Rasmo, D., Signorile, A. and Petruzzella, V. (2012). The oxidative phosphorylation system in mammalian mitochondria. *Advances in Experimental Medicine and Biology*, **942**, 3–37. doi: 10.1007/978-94-007-2869-1_1

Perelman, A., Wachtel, C., Cohen, M., Haupt, S., Shapiro, H. and Tzur, A. (2012). JC-1: Alternative excitation wavelengths facilitate mitochondrial membrane potential cytometry. *Cell Death and Disease*, **3**(11), e430. doi: 10.1038/cddis.2012.171

Perry, S. W., Norman, J. P., Barbieri, J., Brown, E. B. and Gelbard, H. A. (2011). Mitochondrial membrane potential probes and the proton gradient: A practical usage guide. *BioTechniques*, **50**(2), 98–115. doi: 10.2144/000113610

Pyo, J. O., Yoo, S. M., Ahn, H. H., Nah, J., Hong, S. H., Kam, T. I., Jung, S. and Jung, Y. K. (2013). Overexpression of Atg5 in mice activates autophagy and extends lifespan. *Nature Communications*, **4**, 2300. doi: 10.1038/ncomms3300

Rich-Edwards, J. W., Spiegelman, D., Garland, M., Hertzmark, E., Hunter, D. J., Colditz, G. A., Willett, W. C., Wand, H. and Manson, J. E. (2002). Physical activity, body mass index, and ovulatory disorder infertility. *Epidemiology*, **13**(2), 184–190. doi: 10.1097/00001648-200203000-00013

Richani, D., Dunning, K. R., Thompson, J. G. and Gilchrist, R. B. (2021). Metabolic co-dependence of the oocyte and cumulus cells: Essential role in determining oocyte developmental competence. *Human Reproduction Update*, **27**(1), 27–47. doi: 10.1093/humupd/dmaa043

Sharma, S., Sharma, P., Bailey, T., Bhattarai, S., Subedi, U., Miller, C., Ara, H., Kidambi, S., Sun, H., Panchatcharam, M. and Miriyala, S. (2022). Electrophilic aldehyde 4-hydroxy-2-nonenal mediated signaling and mitochondrial dysfunction. *Biomolecules*, **12**(11), 1555. doi: 10.3390/biom12111555

Silva, S. C. A., Braz, G. R. F., do Nascimento, L. C. P., Santana, D. F., da Siva Pedroza, A. A., Silva, T. L. A., Fernandes, M. P., Sellitti, D. F. and Lagranha, C. J. (2019). Influence of maternal protein malnutrition on oxidative stress and regulators of mitochondrial biogenesis in female rat hearts over succeeding generations. *Life Sciences*, **232**, 116579. doi: 10.1016/j.lfs.2019.116579

Skuratovskaia, D. A., Sofronova, J. K., Zatolokin, P. A., Popadin, K. Y., Vasilenko, M. A., Litvinova, L. S. and Mazunin, I. O. (2018). Additional evidence of the link between mtDNA copy number and the body mass index. *Mitochondrial DNA. Part A, DNA Mapping, Sequencing, and Analysis*, **29**(8), 1240–1244. doi: 10.1080/24701394.2018.1436170

Song, J., Zhang, J., Fawzi, W. and Huang, Y. (2020). Double burden of malnutrition among Chinese women of reproductive age and their social determinants. *Nutrients*, **12**(10), 3102. doi: 10.3390/nu12103102

Sutton-McDowall, M. L., Gilchrist, R. B. and Thompson, J. G. (2010). The pivotal role of glucose metabolism in determining oocyte developmental competence. *Reproduction*, **139**(4), 685–695. doi: 10.1530/REP-09-0345

Turathum, B., Gao, E. M. and Chian, R. C. (2021). The function of cumulus cells in oocyte growth and maturation and in subsequent ovulation and fertilization. *Cells*, **10**(9), 2292. doi: 10.3390/cells10092292

Uyar, A., Torrealday, S. and Seli, E. (2013). Cumulus and granulosa cell markers of oocyte and embryo quality. *Fertility and Sterility*, **99**(4), 979–997. doi: 10.1016/j.fertnstert.2013.01.129

WHO Expert Consultation (2004). Appropriate body-mass index for Asian populations and its implications for policy and intervention strategies. *Lancet* (London, England), **363**(9403), 157–163. doi: 10.1016/S0140-6736(03)15268-3

World Health Organization. (2010). *WHO Laboratory Manual for the Examination and processing of Human Semen* (5th edn). World Health Organization Press. Available online: https://www.who.int/publications/i/item/9789240030787.

Zhang, Q., Ji, H., Shi, J., Wang, L., Ding, L., Jiang, Y., Huang, X., Qiu, P. and Li, P. (2021). Digital PCR detection of mtDNA/gDNA ratio in embryo culture medium for prediction of embryo development potential. *Pharmacogenomics and Personalized Medicine*, **14**, 521–531. doi: 10.2147/PGPM.S304747

Zhu, M., Shen, Q., Li, X. and Kang, J. (2020). Removal of peri-ovarian adipose tissue affects follicular development and lipid metabolism. *Biology of Reproduction*, **103**(6), 1199–1208. doi: 10.1093/biolre/ioaa144